JOURNAL OF GUIDANCE, CONTROL, AND DYNAMICS
Vol. 24, No. 3, May–June 2001

Application of Control Structure Design Methods to a Jet Engine

Melker Härefors*
Volvo Aero Corporation, S-461 81 Trollhättan, Sweden

Future jet engines will be more complex with more variables to control to meet increasing demands on functionality. The interaction between the engine and aircraft systems will also increase, with mission-specific control and with control of thrust direction. To utilize the potential of these engines, it is also necessary to use more advanced control concepts than are conventionally used today, utilizing multivariable control techniques. Important parts of a multivariable control design are to select suitable inputs and outputs and how to configure the control laws. This is referred to as control structure design. Some methods to accomplish this have been implemented in MATRIXx and evaluated. A model of a typical jet engine has been used as application in this evaluation. The general impression from this work is that the tested methods and tools are very usable for selection between a large number of possible structures. However, it is essential to combine the use of the methods with application knowledge and understanding of the control objectives.

Nomenclature

$A8$	=	nozzle area
C	=	control sensitivity function
E	=	decentralization error function
FN	=	net thrust, estimated
G	=	plant, jet engine
K	=	controller
$PT21$, $PS21$	=	fan downstream pressure, total and static
$PT3$, $PS3$	=	compressor downstream pressure, total and static
$PT5$	=	turbine downstream pressure, total
S	=	sensitivity function
T	=	complementary sensitivity function
u, y	=	input and output
W	=	weighting function
γ	=	condition number
Δ	=	model uncertainty
δ	=	structure selection bound
Λ	=	relative gain array (RGA) matrix
μ	=	structured singular value
σ	=	singular value
Ψ	=	RGA row sum
ω	=	frequency, rad/s

Subscripts

a	=	additive
ra	=	relative–additive
S	=	sensitivity function
T	=	complementary sensitivity function

Introduction

HISTORICALLY, jet engines have been controlled by hydro-mechanical control systems. Because the engines have become more complex, with more control signals and higher demands on performance and functionality, electronic control systems have been introduced. Today all modern jet engines are controlled by full authority digital engine control systems, or combinations of electronic and hydro-mechanical systems.[1,2] However, the control functions implemented in many of these systems have not changed that much. Simple single-loop control is still the dominant strategy in most systems. Some control signals are open-loop scheduled or are used only for limiting of engine variables. Nevertheless, this works satisfactorily for the engines used today. The trends toward increasingly complex jet engines continue, to meet increasing demands on performance, fuel consumption, and functionality.[3] There are suggestions for variable-cycle engines with variable bypass ratios, variable compressors and variable burners, etc. Many of the engine components might also be actively controlled.[4] The interaction between the engine and aircraft systems will also increase, with mission-specific control and with control of thrust direction. To utilize the potential of these engines, it is necessary to use more advanced control concepts than are conventionally used today. The trend is toward control concepts, often referred to as smart engines. Multivariable controllers are most often at the core of these advanced control concepts.

There have been a large number of research programs investigating multivariable control of jet engines, mainly in the United States and the United Kingdom. The first major program was the F100 multivariable control research program, which used linear quadratic control.[5] In many of the more resent programs, H_∞ have been the preferred design methods (some examples are given in Refs. 6–8). A complete description of H_∞ design for a variable cycle engine is given in Ref. 9. A good review of the multivariable technology programs performed in the United Kingdom can be found in Ref. 10. The H_∞ design technique has also been used in many of the programs dealing with integrated flight-propulsion control, with some examples given in Refs. 11 and 12.

An advanced control research program has been ongoing at Volvo Aero Corporation since 1992: a multivariable jet engine control concept based on H_∞ design.[13] The program has continued with the study of alternative control strategies. This includes use of alternative signals for feedback control, controllers structured in ways other than fully multivariable controllers, and different operational control modes. A survey of control modes and signals used for feedback control in a large number of jet engine multivariable control research programs shows that there are many possibilities. Figure 1 shows an example of a typical jet engine with the usual control signals and some of the possible signals for feedback that have been used in different research programs. There might also be other signals not mentioned here. Many of these signals are also used in control systems for production engines. It is possible to use all of these outputs in a number of different combinations with the available input signals. The problem is to find the combinations of outputs and inputs that are the most suitable for control design, without actually designing controllers for each case.

Control Structure Design

Control structure design (CSD) is an important subproblem in control system design for complex multivariable systems. The

Presented as Paper 99-2943 at the AIAA/ASME/SAE/ASEE 35th Joint Propulsion Conference, Los Angeles, CA, 20–24 June 1999; received 13 August 1999; revision received 2 March 2000; accepted for publication 15 August 2000.

*Research Engineer, Propulsion and Control System Department; also Ph.D. Student, Control Engineering Laboratory, Chalmers University of Technology, 412 96 Gothenburg, Sweden; vac.melh@memo.volvo.se.

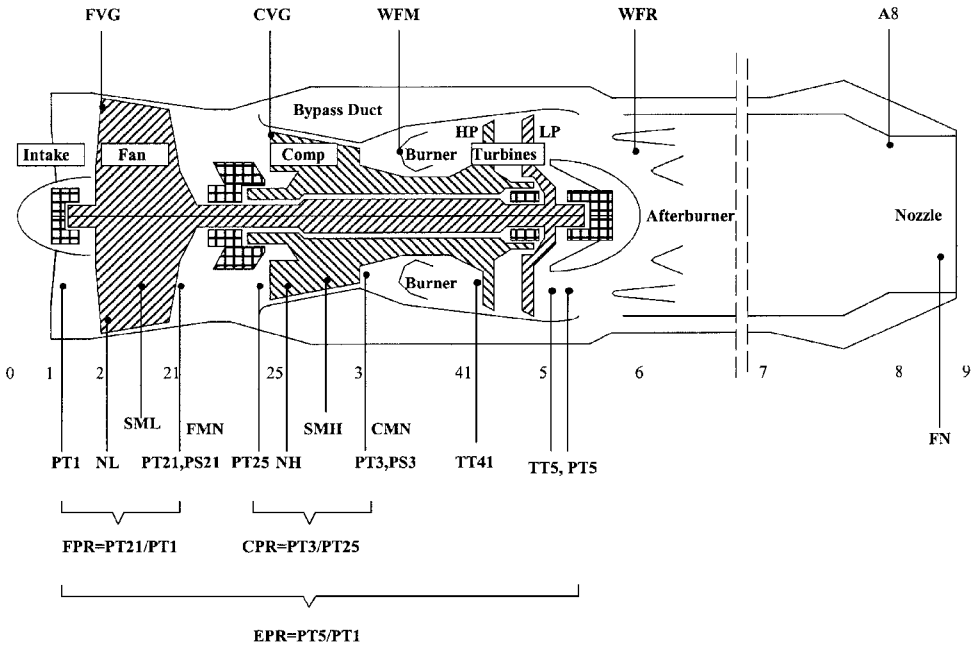

Fig. 1 Jet engine with inputs shown above the engine and the candidate outputs shown below it.

important aspects are to select control modes that best fulfill the control objectives, to select inputs and outputs for these control modes, and to select a control configuration. There are many possible configurations: from fully multivariable control to decentralized control. Efficient methods to do this selection have become more important as the complexity of the engines increases. A survey of possible CSD methods with application to jet engines was done at Volvo Aero Corporation in 1996 and is reported in Ref. 14.

The selection of control structures for jet engines can be divided into three main groups[14]:

1) methods to select control modes based on steady-state sensitivity analysis, which relates all engine performance and safety parameters of interest to the available inputs; 2) methods to select input and output signals from a control design point of view; and 3) methods to select the configuration of control law for the selected inputs and outputs.

The first group of methods selects control modes from an engine steady-state performance point of view, neglecting the dynamics and control design issues. The selected outputs are assumed to be perfectly controlled by the available inputs.[15] This is the approach generally used to select control modes for jet engines today. A tool for this approach has previously been developed and evaluated at Volvo Aero Corporation.[16] The main drawback, from a control perspective, is that this method does not give any information about how well the outputs actually can be controlled or about the interaction between different control loops. For that sort of analysis, the methods belonging to groups two and three can be used.

The work at Volvo Aero Corporation has continued by developing CSD tools for some selected methods belonging to these two groups. The aim of this work has mainly been to evaluate the methods to better understand the possibilities to predict the controller performance without actually designing controllers for each structure. Three methods have been used to select a set of candidate inputs and outputs for a multivariable controller. These methods are used consecutively to reduce the set of possible structures gradually. Four different methods have then been used to search for decentralized or block-decentralized control configurations for these structures. These are alternative methods with different approaches to find suitable configurations. The methods are briefly summarized later. The names of some of the methods are suggested by Volvo Aero Corporation. For a full description, the interested reader is referred to the original papers. The application and evaluation of the methods are more thoroughly described in Ref. 17. For use in a real application, these methods should of course be used in conjunction with, and as a complement to, the steady-state sensitivity method. However, in this paper only the control theoretical methods are considered.

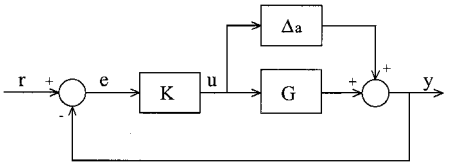

Fig. 2 Framework for analysis of inputs and outputs with RSCN method.

Methods for Input/Output Selection

The first of the tested methods was proposed in Ref. 18 and is based on a criterion for robust stability and the condition number for the system. This method, robust stability by the condition number (RSCN), could be used for design-specific as well as design-independent evaluation of different input/output sets. For the design-specific evaluation, the criterion gives necessary and sufficient conditions for robust stability; whereas for the design-independent case, this is relaxed for a controller to exist that achieves necessary conditions for robust stability. The method is based on the condition for robust stability arising from the small gain theorem.[19] Figure 2, with a controller K, a plant G, and an unstructured additive uncertainty Δ_a, shows the framework for the analysis.

The small-gain theorem states that if the nominal closed-loop system is stable and the uncertainty can be described by a stable transfer function, then the closed-loop system will remain stable for all uncertainties such that the resulting loop gain is less than unity. Based on this, a necessary test condition for robust stability is derived, with the plant condition number $\gamma(G)$:

$$\gamma(G) < 1/\delta_{\text{ra}}(1-\sigma_s) \qquad \forall\omega \le \omega_s \tag{1}$$

The designer should specify how much of the disturbances should be attenuated, σ_s, for frequencies below ω_s and what the upper level of additive-relative uncertainty $[\bar{\sigma}(\Delta_a) \le \delta_a = \delta_{\text{ra}}\bar{\sigma}(G)]$ is that can be tolerated. A scale-independent version of this criterion is also developed. For this, a lower bound on the condition number calculated from relative gain array (RGA)[20] is utilized:

$$2\max\{\|\Lambda(G)\|_1, \|\Lambda(G)\|_\infty\} - 1 < 1/\delta_{\text{ra}}(1-\sigma_s) \qquad \forall\omega \le \omega_s \tag{2}$$

where $\|\Lambda(G)\|_1$ and $\|\Lambda(G)\|_\infty$ are the maximum column and row sums of absolute values of the RGA, respectively.

The next selection method is simply to select structures without any right-half-plane (RHP) zeros. The existence of RHP zeros in a system is likely to limit the performance of any feedback controller. This will cause a problem in the control design if a RHP zero is located inside the range of the desired open-loop bandwidth for disturbance rejection.[19,21] Because different input/output sets will have different zeros but the same poles, one input/output selection method is to choose input and output sets without any RHP zero within the desired bandwidth.

The last method for comparing different input/output sets is to study the controllability and observability of the system. This can be done by calculating the controllability and observability gramians. The Hankel singular values for the system calculated from these give a measure of the joint controllability and observability of a system. This property can be used to select a suitable input/output set because high controllability and observability would be beneficial in the control design.[22]

Methods for Control Configuration Selection

RGA

The RGA, first proposed in Ref. 23, is the most well-known method for configuration selection. Several authors have contributed to development and interpretation of RGA, for example, see Refs. 22 and 24–28. RGA was originally defined for steady-state operation to show how a transfer function for one loop in a multivariable system was effected by controllers in the other loops. This is a controller-independent measure of the multiplicative perturbation of the gain for one loop caused by the other loops. The RGA is defined as the matrix with all loop perturbations. For a system with n inputs and n outputs, the relative gain between an input u_j and an output y_i is the ratio between two gains: The steady-state gain between u_j and y_i when no control is applied to the system and the gain between the same variables when feedback control involving all other inputs and outputs is applied to the system under perfect steady-state control. This is mathematically expressed as

$$\lambda_{ij} = \left(\frac{\partial y_i}{\partial u_j}\right)_{u_k=0,k\neq j} \Bigg/ \left(\frac{\partial y_i}{\partial u_j}\right)_{y_l=0,l\neq i} \tag{3}$$

This calculation can easily be made in matrix form, where frequency dependence also is introduced:

$$\Lambda(s) = G(s) * G(s)^{-T} \tag{4}$$

In this equation, $G(s)^{-T}$ is the transpose of the plant with the inverse of each element, and $*$ is the element-by-element product.

There are some rules for the use of the RGA for configuration selection. These are summarized as follows:

1) Avoid configurations with large RGA elements, in particular at frequencies near the crossover region.

2) Avoid configurations with negative RGA elements at steady state if decentralized control with integral action is to be used.

3) Avoid configurations with different signs on the RGA elements for low and high frequencies.

4) Prefer configurations with RGA diagonal elements close to one, in particular at frequencies near the crossover region.

The RGA as defined here are restricted to square systems. The definition can also be extended to nonsquare systems utilizing the pseudoinverse of the system.[22]

Block Relative Gain (BRG)

The next method is an extension to RGA proposed in Ref. 29 and called block relative gain (BRG). This method can also handle block-decentralized controller configurations. With the BRG concept, it is possible to identify subsystems with strong interaction that need multivariable controllers, while the interaction with other subsystems is low. In this way it is possible to select a control configuration with one or several multivariable or single controllers, instead of fully centralized or decentralized controllers. The BRG is calculated from the ratio of two transfer function matrices instead of scalar gains as for the RGA: the matrix with no control applied to any subsystem and the matrix with all other subsystems under perfect control. The (left) BRG for the subsystem $G_{11}(s)$ of $G(s)$ can be calculated as

$$\mathrm{BRG}_l(s) = \left[\left.\frac{\partial y_1}{\partial u_1}\right|_{\substack{u_2=0\\F=0}}\right] \cdot \left[\left.\frac{\partial y_1}{\partial u_1}\right|_{\substack{y_2=0\\F_1=0,F_2=I}}\right]^{-1}$$

$$= [G(s)]_{11}[G(s)^{-1}]_{11} \tag{5}$$

where $F=0$ means that all loops are open and $F_1=0$ and $F_2=1$ mean that only the loop for subsystem two is closed. The BRG_l gives a measure of the performance degradation due to interaction with other subsystems. A good control configuration is said to be achieved if all of the BRGs corresponding to the diagonal blocks of G are close to the identity matrix. If the BRG is exactly the identity matrix for a certain subsystem, the closed-loop response for this subsystem is as if it was isolated from the rest of the system and influenced only by its own controller. The analysis can be simplified by studying only the diagonal elements of the BRGs, as a first step. The diagonal elements of a BRG can easily be obtained from the RGA as the partial row sum for the subsystem RGA. When this initial study has been performed, the complete BRGs can be calculated only for those configurations where the diagonal elements fulfill the requirements. The control configuration selection is accomplished by searching for a block partition where all of the BRGs of different dimensions corresponding to the diagonal blocks of G are close to an identity matrix. The designer has to define a selection criterion, that is, what degree of interaction between the subsystems can be tolerated.

Block-Decentralized Performance Degradation (BDPD)

This method was proposed in Ref. 18 and measures the performance degradation due to use of (block-) decentralized controller configurations. The block-decentralized performance degradation (BDPD) concept is a way to specify the ideal nominal performance and to measure how much this is degraded due to interactions that are not taken into account in the controller design. The nominal performance of the closed-loop system is measured by the complementary sensitivity function T:

$$T(s) = G(s)K(s)[I + G(s)K(s)]^{-1} \tag{6}$$

The controller K is a block-diagonal controller, and G is the control object in the same way as for the BRG in Fig. 3. The interaction between the subsystems controlled by the block-diagonal controller, and not considered in the controller design, is described by G_{12} and G_{21}. Thus, the controller is designed for the block-diagonal system $\bar{G} = \mathrm{diag}\,(G_{11}, G_{22})$. The ideal complementary sensitivity function $\bar{T}$ will, therefore, be considered the as one calculated for this block-diagonal control object. The extent to which T differs from the ideal will characterize the impact of the crossfeed on the closed-loop performance. The maximum value of the relative difference is a measure of performance degradation, with δ_T as the maximum allowed degradation. The control configuration selection criterion is as follows:

$$\frac{(1-\sigma_T)\bar{\sigma}[E(j\omega)]}{1+(1-\sigma_T)\bar{\sigma}[E(j\omega)]} \leq \delta_T \quad \forall\omega \geq \omega_T$$

$$E = (G - \bar{G})G^{-1} \tag{7}$$

The ideal closed-loop system performance is determined by choosing the parameters ω_T and σ_T, such as $\bar{\sigma}(\bar{T}) \leq \sigma_T$, where

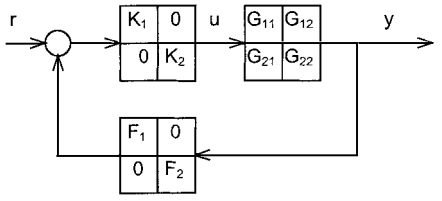

Fig. 3 Framework for two-block control structure analysis with the BRG method; two-block decentralized configuration shown as an example.

$\sigma_T < 1 \quad \forall \omega \geq \omega_T$. This selection criterion is dependent on the input and output scaling because G is included in the measure. It is possible to make it scale independent by using the concept of the RGA. The interaction measure between subsystems can be obtained as the RGA complementary row sum $\bar{\Psi}_i$. The scale-independent selection criteria then become

$$\frac{(1-\sigma_T)|\overline{\Psi(j\omega)}|_{\max}}{1+(1-\sigma_T)|\overline{\Psi(j\omega)}|_{\max}} \leq \delta_T \qquad \forall \omega \geq \omega_T \tag{8}$$

Block-Decentralized Robust Stability (BDRS)

Finally, the last method, proposed in Ref. 30, also measures the performance loss due to decentralization. A criterion based on the structured singular value of the error due to decentralization is used for stability analysis. The structured singular value can be used as an interaction measure for feedback systems with diagonal or block-diagonal controllers. In addition to the prediction of the stability of the (block-) decentralized closed-loop system, the BDRS concept also gives a measure of the performance loss due to the decentralized control structure.

In the same way as described for the BDPD method, an ideal complementary sensitivity function $\bar{T}(s)$ will be considered as the one calculated for a control object with the same block-diagonal structure as the controller. Now an uncertainty matrix is defined as a multiplicative output uncertainty, which can be viewed as a multiplicative perturbation on the ideal complementary sensitivity function:

$$E(s) = [G(s) - \bar{G}(s)]\bar{G}(s)^{-1} \tag{9}$$

From this, the following robustness condition for the closed-loop system is defined:

$$\bar{\sigma}[\bar{T}(j\omega)] < \mu^{-1}[E(j\omega)] \qquad \forall \omega \tag{10}$$

The μ depend on the structure imposed on the control object G. For stability, the diagonal blocks $\bar{T}_{ii}$ have to be constrained by the inverse of the μ for the multiplicative error of the control object. However, to calculate the diagonal blocks $\bar{T}_{ii}$, we have to design a controller. This makes it unsuitable as a tool for control configuration selection, at least in the initial state. Imposing some desirable properties for the closed-loop system can solve this. A requirement on the ideal closed-loop system can be specified in the form

$$\bar{\sigma}[\bar{T}(j\omega)] \leq \delta_T(\omega) \qquad \forall \omega \tag{11}$$

that is, a specification on the maximum gain for the closed-loop system, for different frequencies. This gives the design-independent criterion for robust stability as

$$\mu^{-1}[E(j\omega)] > \delta_T(\omega) \qquad \forall \omega \tag{12}$$

One limitation with these conditions, as well with the other configuration selection methods, is that they give equal preference to all of the control loops. For real applications, it is often necessary to separate the requirements for the different loops. One way to circumvent this problem is to introduce a weighting function matrix $W(s)$, with a block-diagonal structure equal to that of $\bar{T}$. The sufficient robustness condition then becomes

$$\bar{\sigma}[W^{-1}(j\omega)\bar{T}(j\omega)] < \mu^{-1}[E(j\omega)W(j\omega)] \qquad \forall \omega \tag{13}$$

A proper weighting matrix will express a performance constraint imposed on one or more of the control loops in $\bar{T}$ due to, for example, constraints in the manipulated variables or the physics of the plant.

Application to the Jet Engine

The CSD methods are now used to select suitable control structures for the jet engine. The available inputs are fixed for this application, but there are a large number of possible outputs, shown in Fig. 1. All of these outputs are possible to use, and have been, in a number of different combinations with the available input signals. The problem is to find the combinations of outputs and inputs that are the most suitable for control design, without actually designing controllers.

A detailed nonlinear simulation model of the RM12 jet engine for the Swedish fighter aircraft JAS 39 Gripen has been used in this study. This is a typical two-spool military engine with afterburner, as shown in Fig. 1. The study presented in this paper is performed for a medium thrust operating point (power level angle 60 deg) where the afterburner is not used, that is, only four of the five inputs are used. The model has been linearized in this operating point for the CSD analysis. The analysis should of course be repeated for each design point because the couplings change over the engines operating range. The linear model utilized was also reduced from order 32 to order 17 for numerical reasons before being used for the CSD. A more detailed description of the engine, the nonlinear model, the linearization procedure, and the model reduction method can be found in Ref. 13.

Traditional in jet engine control systems today, only one main fuel (WFM) or two (WFM and $A8$) of the controls are used for feedback control, with the fan vanes (FVG) and compressor vanes (CVG) open-loop scheduled. However, some studies indicate improvements by using also the fan and compressor guide vanes for feedback control. In Ref. 4, improved handling of pressure disturbances was reported, and in Ref. 10 fast response modes with nonconventional usage of CVG have been evaluated. Based on this a control design using all inputs for closed-loop control was considered in this paper. Because most of the CSD methods used require square systems, four of the outputs should be selected. This gives as many as 495 candidate structures, when all combinations are considered. In Ref. 17, more traditional 2×2 systems are evaluated. An interesting extension would be to use these methods to analyze fault-tolerant degraded control modes for sensor or actuator failures. Some studies in this direction have also been performed.

Some very basic control requirements were used for the evaluation of the CSD methods. The requirements were that there should be integral action in all control loops, the bandwidth should be around 10 rad/s, and there should be rolloff for higher frequencies. In practice, there are of course a number of additional requirements and restrictions on the measured outputs, on other performance and safety parameters, and on the control inputs.[17]

Selection of Outputs

The first step in reducing the set of possible control structures was done by using the scale-independent robust stability by the condition number (RSCN) method. The requirement that disturbances should be attenuated by 3 dB was used. Two different bandwidth frequencies were tested: 2 and 5 rad/s, selected based on the previous design study.[13] All structures were tested for a range of bounds for the additive–relative uncertainty measure. The result from this test is summarized in Table 1.

From Table 1, it can be seen that the number of possible structures is decreased as the requirements on bandwidth and uncertainty are increased. The number of possible 4×4 structures decreases from 495 to as few as 56. There are still too many possible structures left after this first selection. The next step is to find an appropriate scaling of the inputs and outputs and apply the stronger scale-dependent test condition to the remaining set. Note that the selection should not be done with too high requirements in this scale-independent test. A system that seems to be relatively bad in the scale-independent test can be better than other systems when scaled properly. The scaling might change the picture, and it is then important to have the potentially suitable structures in the selected set. Because the scale-independent test is based on a calculation of the lower bound for the condition number, a system can not be better then this whatever scaling is used. The set selected for further evaluation

Table 1 Number of structures that pass first test

Frequency, ω_s	δ_{ra} 0.25	0.5	1.0
2	359	241	106
5	350	224	56

with the stronger scale-dependent criteria should, therefore, contain all systems that fulfill a minimum requirement for a scaled system. That is, this first test should not be used to compare different structures because the scaling might alter this comparison dramatically; rather it should be used to take away systems that never can fulfill the minimum requirement. The selection done at this stage was to discard all structures that did not fulfill the requirement on 25% additive–relative uncertainty at 5 rad/s; then 350 structures are left for further analysis.

The next step was to apply the scale-dependent version of RSCN to the selected structures. It is essential how the scaling of inputs and outputs is done. There are a number of different approaches, and the one selected in this study is to scale according to smallest significant deviation of interest.[4] However, this might be done in a number of ways, and the outcome from the RSCN selection depends on how the scaling is done. The same test requirements were used also for this step, and the result is summarized in Table 2.

As can seen, there are considerable fewer structures that pass this stronger scale-dependent test. An inspection of the structures that passed this test showed that a suitable large set to evaluate further might be the structures that pass the test for $\delta_{ra} = 0.5$ at $\omega_s = 2$. These all fulfill the necessary condition for robust stability, with a relative–additive uncertainty of 50%. The reason the requirement was not increased even further was the uncertainty of how the scaling should be selected to best reflect the objectives for control design. With this choice of robustness requirement, the risk that possible structures will be rejected due to a bad choice of scaling is low.

The set of possible structures was further reduced by removing the structures with RHP zeros in a frequency range of interest. The selection done here was to remove RHP zeros below 100 rad/s. It was found that as many as 18 of the 36 selected structures had such RHP zeros. Left for further selection is 18 structures. The last step in the structure selection was to analyze the joint controllability and observability properties. A measure of this is the magnitude of the Hankel singular values (HSV). A structure with higher hsv might be more suitable for feedback control. Because there is no finite HSV limit when a structure is unsuitable for control, it is not clear how structures should be selected based on this. Therefore, this information is used together with application of knowledge on selection of the most suitable structures. One choice made at this point was to use only the structures with measured outputs and the ones that have the maximum HSV above the median of all structures in the set. With this choice, only four structures remain. Table 3 shows these structures, along with the test values from the RSCN method.

Table 2 Number of structures that pass stronger scale-dependent test

Frequency, ω_s	δ_{ra} 0.25	0.5	1.0
2	131	36	0
5	96	13	0

Table 3 Remaining structures

Outputs	Lower bound	Condition number	δ_{ra}
NL, NH, FPR, CPR	3.39	6.45	0.53
NL, NH, FPR, TT41[a]	2.68	5.69	0.60
NL, NH, FPR, EPR	2.61	5.05	0.68
NL, NH, FPR, TT5	2.52	5.27	0.65

[a]Turbine inlet temperature, estimated.

Selection of Control Configuration

The next step was to analyze these potential structures to see if fully multivariable controllers have to be used or if simpler decentralized or block-decentralized configurations could be found. This is done via the four described methods. The result is presented only for one structure in this paper, the structure with low-pressure rotor speed (NL), high-pressure rotor speed (NH), fan pressure ratio (FPR) (PT21/PT1), and turbine downstream temperature (TT5) as outputs.

First the RGA analysis was done. The analysis was performed at two frequencies: at steady state and at an anticipated crossover frequency at 10 rad/s. The outputs are ordered to make the RGA as diagonal dominant as possible at 10 rad/s. When the RGA is calculated at steady state with the same output order, the diagonal dominance is lost, which shows that there are other couplings of importance at steady state other than at 10 rad/s. This is seen by plotting the RGA elements as a function of frequency (Fig. 4). This analysis

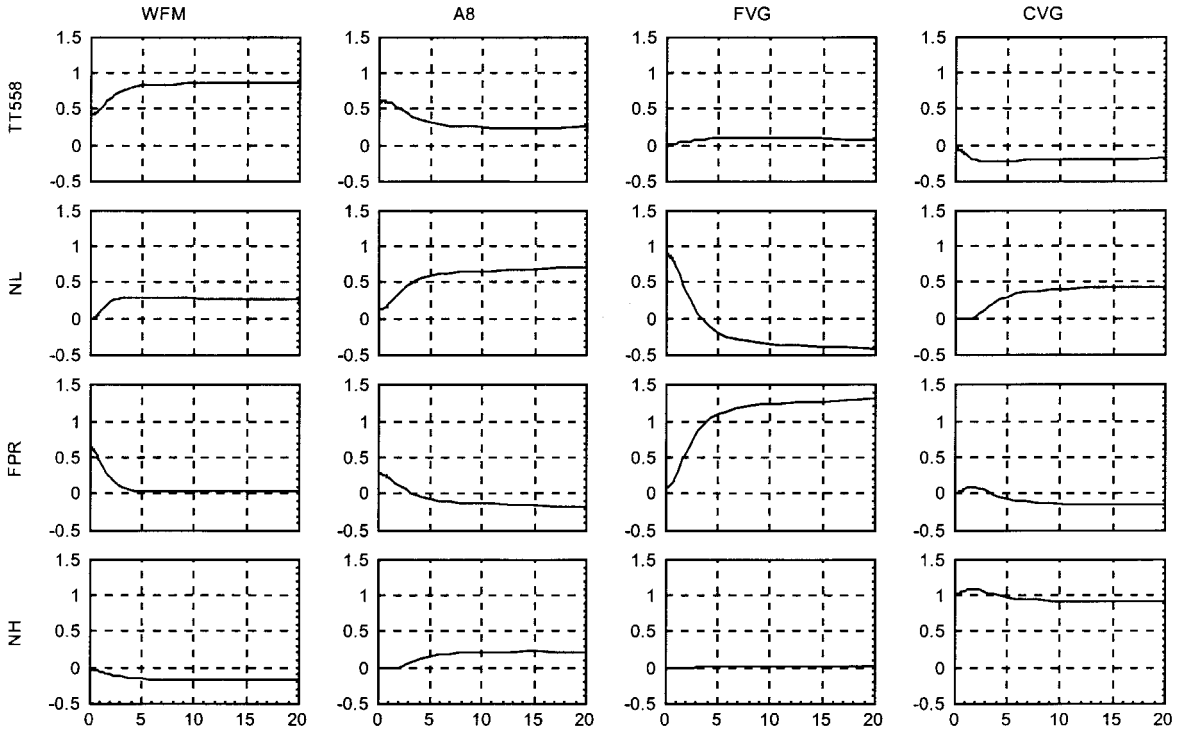

Fig. 4 Result from frequency-dependent RGA analysis, with input–output ordering at 10 rad/s.

Table 4 Steady-state analysis (BRG method)

	2 × 2 + 2 × 2 Configuration				2 × 2 + 1 × 1 + 1 × 1 Configuration			
Parameter	WFM	*A*8	FVG	CVG	WFM	*A*8	FVG	CVG
FPR	0.92	0.00	——	——	0.92	0.00	——	——
TT5	0.22	1.02	——	——	0.22	1.02	——	——
NL	——	——	0.91	0.06	——	——	0.90	——
NH	——	——	0.02	1.03	——	——	——	1.03

Table 5 Analysis at 10 rad/s (BRG method)

Parameter	WFM	*A*8	FVG	CVG
NL	0.96	0.17	——	——
TT5	1.51	1.10	——	——
NH	——	——	0.95	0.20
FPR	——	——	1.29	1.11

Table 6 Scale (in) dependent test (BDPD method)

	δ_T			
Configuration	0.5	0.4	0.3	0.2
Four 1 × 1	(24) 4	(24) 1	(24) 0	(3) 0
2 × 2 + 1 × 1 + 1 × 1	(72) 3	(72) 1	(72) 1	(12) 0
2 × 2 + 2 × 2	(18) 0	(18) 0	(18) 0	(5) 0
3 × 3 + 1 × 1	(16) 0	(16) 0	(16) 0	(6) 0

clearly show how the interactions change with frequency and that it is not possible to find a decentralized configuration for this structure when following the RGA rules. The next step was to try to find any block-decentralized structures using BRG. With this method the analysis was also performed at steady state and at 10 rad/s. All possible configurations are searched for by using the relation between RGA and the diagonal elements of the BRG. Then the complete BRGs are calculated only for these configurations. One block-decentralized 2 × 2 + 2 × 2 and one 2 × 2 + 1 × 1 + 1 × 1 configuration was found at steady state (Table 4). These two BRGs fulfill all of the rules for block-decentralized configurations at steady state. When the analysis was performed at 10 rad/s, another block-decentralized configuration was found. The complete BRG for this configuration was calculated, with the results shown in Table 5. The diagonal elements are as expected, but there are also large off-diagonal elements in both blocks. This indicates that there will be interaction between the blocks; thus, this is not a suitable configuration for block-decentralized control. There are also different blocks at steady state and at 10 rad/s, making it difficult to find a block-decentralized controller.

The BDPD method was used next. This method has two versions, one scale independent and one scale dependent. Both versions were tested. The test was performed for the frequency range 5–20 rad/s. A requirement of 3-dB damping at the bandwidth was used. A set of different performance degradation requirements ($\delta_T = 0.2, 0.3, 0.4,$ and 0.5) were tested. The number of structures that passed each test criterion are shown in Table 6, with the scale-independent test shown parentheses. Almost all configurations passed the scale-independent test, even for high requirements on performance degradation. It seems that this measure is too weak to of practical use for configuration selection. When the stronger scale-dependent criterion was used, almost no configurations were accepted. The few that were accepted did not seemed to be realistic from a physical point of view.

The last method to test is the BDRS. This test was first done at steady state and at 10 rad/s. The requirement selected was that $\mu^{-1}(E)$ is larger than 1 at steady state and larger than 0.7 at 10 rad/s. Then the configurations were tested in the frequency region where resonance peaks are possible. The requirement in this region was set to 1.2. The number of structures that passed each test criterion is shown in Table 7. There are a number of configurations that fulfill the criterion either at steady state or at 10 rad/s. Only one fulfills both criteria. This is the 3 × 3 + 1 × 1 configuration, with

Table 7 Steady-state and 10-rad/s BDRS test

Configuration	Steady-state structures	10 rad/s structures
Four 1 × 1	——	1
2 × 2 + 1 × 1 + 1 × 1	1	5
2 × 2 + 2 × 2	1	1
3 × 3 + 1 × 1	2	3

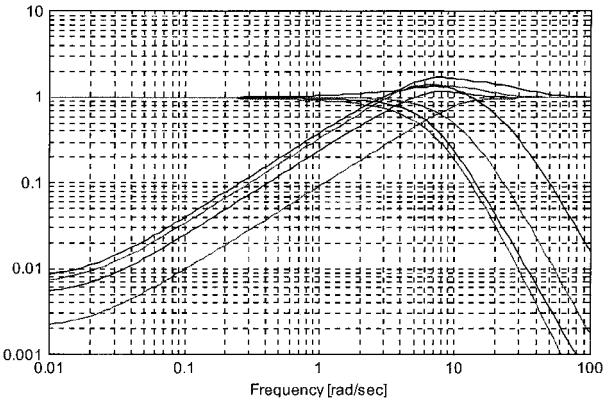

Fig. 5 Singular values of *S* and *T* for the full multivariable control design.

the 3 × 3 block {NL, FPR, TT5}/{WFM, *A*8, FVG} and the 1 × 1 block {NH}/{CVG}.

As a further analysis, the weighted version of BDRS was also tested. With this extension is it possible to separate the requirements for the different control loops. This was used to release the requirement on integral action for one or two of the outputs. This was performed for those structures that passed the preceding test at 10 rad/s, where the requirement for integral action has no impact. To test all possible combinations of integral actions, it is necessary to repeat the calculations for each tested block structure, with different structures of the weighting matrix. For example, with a 2 × 2 + 2 × 2 block structure, there are six possible combinations of integral action for two outputs. All combinations are tested in this study to cover all possibilities. The first 2 × 2 block for this structure is {FPR, TT5}/{WFM, FVG} and the second block is {NL, NH}/{*A*8, CVG}. The four approved combinations of integral actions are {FPR, TT5}, {FPR, NH}, {TT5, NH}, or {NL, NH}.

Control Design and Evaluation

Controllers were designed for a number of different structures to evaluate the predictions from the CSD methods. The same design methodology as previously used at Volvo Aero Corporation based on H_∞ was used for this. The mixed sensitivity design approach[19,31] was used, where the sensitivity *S*, complementary sensitivity *T*, and control sensitivity *C* functions are minimized. This approach for the jet engine control is further described in Refs. 13 and 17.

The control design for the structure with NL, NH, FPR, and TT5 as outputs is described in this section as an example. Both fully multivariable as well as block-decentralized control designs are done. Figure 5 show the sensitivity functions *S* and *T* for the fully multivariable design. The design is satisfactory; there are integral actions for all control loops (*S* is small for low frequencies), there is good rolloff (*T* is small for high frequencies), and there are no high peaks in the crossover region.

This structure was further evaluated via simulation with different additive uncertainties. The simulation setup was similar to that shown in Fig. 2, and steps were applied to all references at 0.5 s. This structure was approved by the design-independent RSCN selection criterion with an upper bound of the relative–additive uncertainty of $\delta_{ra} = 0.65$. The maximum singular value for the engine at this operating point is 1.3, which means that the bound on the additive uncertainty is $\delta_a = 0.85$. However, this bound stems from the necessary criterion for stability. There are several steps of approximations to derive this design-independent criterion. When the controller is designed we could apply the stronger necessary and

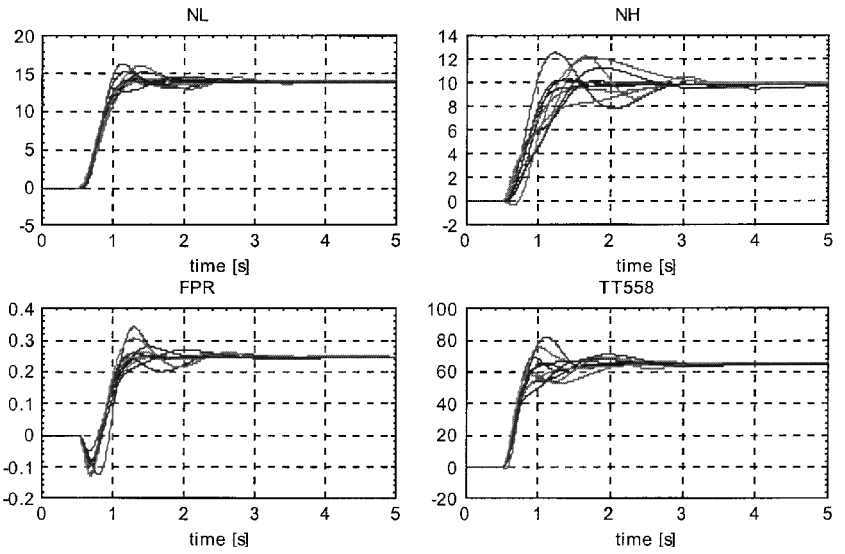

Fig. 6 Simulation with unstructured additive uncertainty for the full multivariable design.

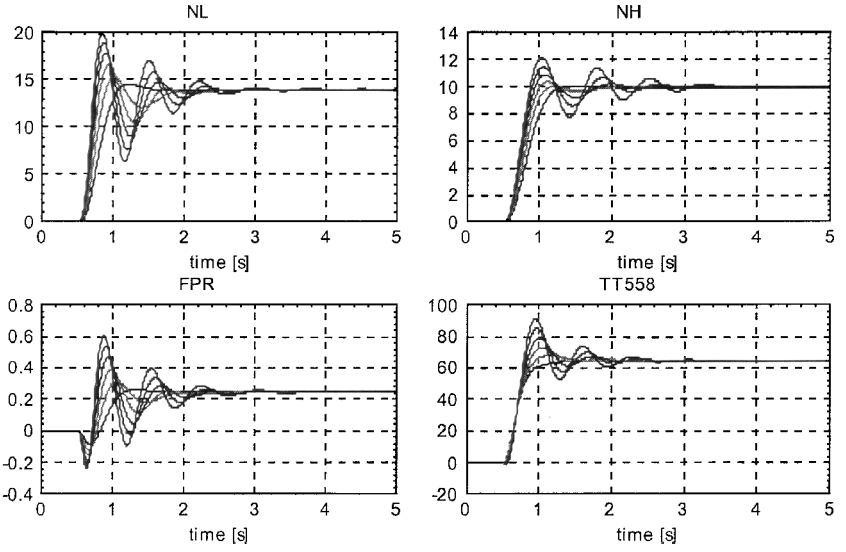

Fig. 7 Simulation with structured additive uncertainty for the full multivariable design.

sufficient criterion instead. The bound on the additive uncertainty is then decreased to $\delta_a = 0.25$. This means that the design-independent selection criterion is more than three times too optimistic.

Monte Carlo simulations were made with randomly generated unstructured uncertainties to evaluate if this holds. For each uncertainty level, 100 different systems were simulated. It was possible to increase the maximum singular value of the uncertainties to 0.3 with maintained stability. Figure 6 show simulations with 10 such uncertainties. Some uncertainties that destabilized the system were found when the bound was increased to 0.35. This simulation result agrees well with the prediction from the RSCN method when using the design-dependent criterion. However, it is interesting to compare the design-independent criterion used for structure selection. This criterion predicted stability for uncertainties with maximum singular values up to 0.85 instead of 0.30 as tested here. Another aspect of this is that the uncertainty used in the RSCN selection is unstructured. This means that the system will be robust to possibly unrealistic uncertainties that can not occur in practice.

An attempt was made to test more realistic uncertainties with structures similar to the design model. This was done by using a model from an adjacent operating point as an additive uncertainty and varying the gain. Simulations with such uncertainties with maximum singular values ranging from 0 to 3 are shown in Fig. 7, which clearly shows that the system is stable for uncertainties up to 10 times the size, when a particular structure is assumed. In this sense, the RSCN condition is too conservative.

Block-decentralized control design has also been tested for this structure. Note that no decentralized configuration was approved by all of the selection methods. A design for a $2 \times 2 + 2 \times 2$ block configuration is shown here as an example. The first block is {NL, NH}/{$A8$, CVG} and the second block is {FPR, TT5}/{WFM, FVG}. This configuration was approved only by the scale-independent version of BDPD method. In addition, it was approved by the weighted BDRS method when the requirement for integral action was removed from NL.

The control design was done independently for these two blocks and then merged to a block decentralized controller. The designs for each block was satisfactory, and the simulation for each block behaved as expected. However, when analyzed with the block-decentralized controller, the performance is drastically degraded due to interaction between the blocks. The sensitivity functions for this system are shown in Fig. 8. These could be compared to the fully multivariable design in Fig. 5. Note especially how the sensitivity functions are changed in the important crossover region. A simulation was also performed for this configuration and the result is shown in Fig. 9. Even without any uncertainty, the system is close to instability.

This confirms the result from the configuration selection methods; this configuration is not suitable for decentralized control. A last test was done where the requirement of integral action was removed from NL. This modification was proposed by the weighted BDRS method. The simulation of this system is shown in Fig. 10.

The prediction from the BDRS method agrees with the simulation result; the stability is improved compared to the case with integral action for all outputs. The overall behavior of the step response, however, is not satisfactory. The performance degradation due to the block-decentralized structure is considerable, and in practice such a response should not be accepted. Compare this with the simulations for the fully multivariable configuration. These effects could not be predicted by the BDRS method that only concerns the stability. The BDPD method rejected this configuration due to high-performance degradation around and above the bandwidth.

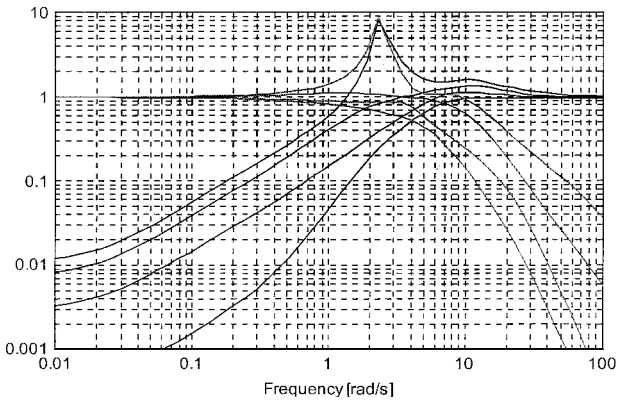

Fig. 8 Sensitivity functions for complete system with block-diagonal controller.

Conclusions

The tools for CSD have been used to evaluate a large number of candidate control structures and (block-) decentralized structures. The predictions from these methods have been thoroughly evaluated and compared to an actual design for some selected structures. The general impression is that the methods and the tools are very useful for selection between a large number of structures. It was possible to find structures that were more suitable for control design and to reject structures that were less suitable. This is difficult to do based only on application knowledge. However, it is essential to combine the use of the methods with a great deal of application knowledge and understanding of the control objectives. The methods should not be used blindly; rather they should be used to assist in the selection process. In the following, some comments and observations from the evaluation of the methods are given.

The observations done in the control design with the fully multivariable structures agree well with the result from the RSCN method; the structure that was approved also gave a good design result. A general observation is that the selection criterion in RSCN with the design-independent necessary condition tends to be very optimistic. Usually this condition allowed 2–3 times higher uncertainty levels than the stronger design-specific necessary and sufficient condition. Another observation that makes the selection more conservative is that the structures were much more robust to uncertainties with a

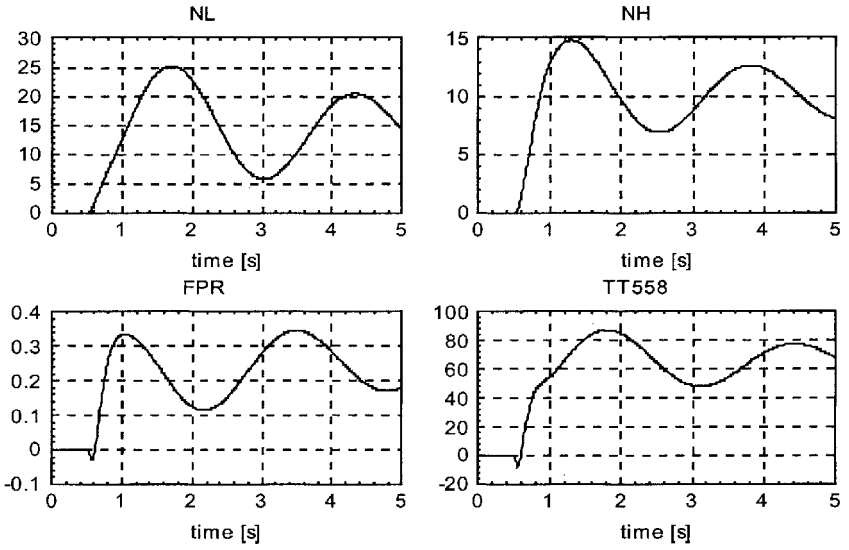

Fig. 9 Simulation of complete system with block-diagonal controller.

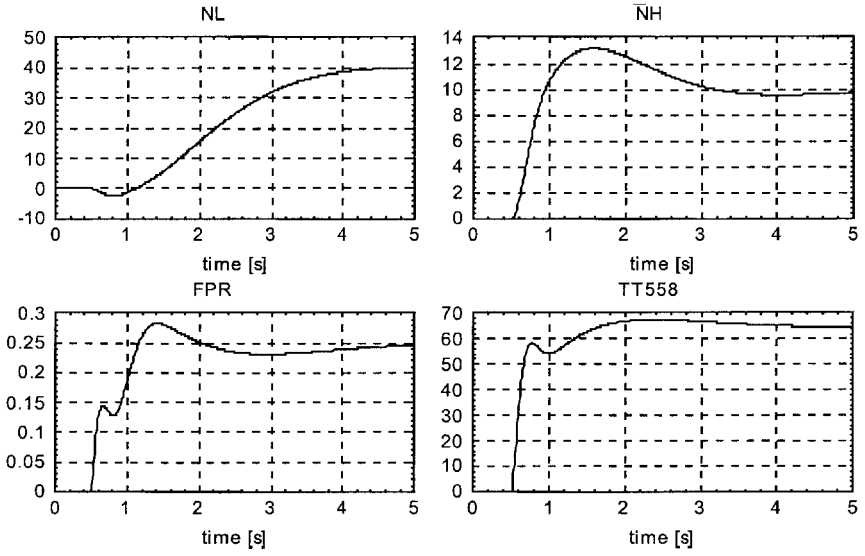

Fig. 10 Simulation of complete system with block-diagonal controller, without NL integral control.

structure similar to the design model. When uncertainties in the form of a model from another operating point were used, the size of these uncertainties could be as much as 5–10 times higher than for the unstructured uncertainties. The reason is that although the maximum singular values are higher, there are fewer and more realistic uncertainties in phase and signal directions.

It turned out to be more difficult to find any good decentralized or block-decentralized configurations for the selected structures. No configuration was approved by all of the tested methods. The result from the control design and the simulation evaluation showed that none of the analyzed block-decentralized configurations performed well. This agrees with the main results from the selection methods.

One of the major limitations of all the studied CSD methods is that only linear analysis can be done. There is, for example, no way to specify an allowed range for the control signals. As noticed in the evaluation, several of the approved structures required control signals beyond the limitations of the actuators. This could possibly have been avoided with another scaling of the inputs, but it is not appropriate to select scaling for each structure, or to use iterative search for suitable scaling.

Acknowledgments

This work was supported by the Swedish Defence Material Administration and the Swedish National Flight Research Program, which is hereby acknowledged.

References

[1]Scoles, R. J., "FADEC—Every Jet Engine Should Have One," Society of Automotive Engineers, SAE Paper, 1986.

[2]Skira, C. A., and Agnello, M., "Control Systems for the Next Century Engines," *Journal of Engineering for Gas Turbines and Power*, Vol. 114, Oct. 1992, pp. 749–754.

[3]Ruffles, R. L., "Innovation in Aero Engines," *Aeronautical Journal*, Dec. 1996, pp. 473–484.

[4]Przybylko, S. J., "Active-Control Technologies for Aircraft Engines," AIAA Paper 97-2769, 1997.

[5]De Hoff, R. L., Hall, W. E., Adams, R. J., and Gupta, N. K., "F100 Multivariable Control Synthesis Program," Vol. I–II, 1–2, Air Force Aero Propulsion Lab., AFAPL-TR-77-35, 1977.

[6]Samar, R., and Postlethwait, I., "Multivariable Controller Design for a High Performance Aero-Engine," *Proceedings of the IEE Control Conference '94*, 1994, pp. 1312–1317.

[7]Frederick, D., Garg, S., and Adibhatla, S., "Turbofan Engine Control Design Using Robust Multivariable Control Technologies," AIAA Paper 96-2587, 1996.

[8]Adibhatla, S., Garg, S., Collier, G., and Zhao, X., "H_∞ Control Design for a Jet Engine," AIAA Paper 98-3753, 1998.

[9]Adibhatla, S., Garg, S., Collier, G., and Zhao, X., "Advanced Multivariable Technology for Engine Controls (AMTEC)," Final Rept. NASA CN NAS3-26617, 1998.

[10]Dadd, G. J., Sutton, A. E., and Grieg, A. W. M., "Multivariable Control of Military Engines," Propulsion Technology Dept., Defence Research Agency, Farnborough, UK, 1995.

[11]Garg, S., "Robust Integrated Flight/Propulsion Control Design for a STOVL Aircraft Using H_∞ Control Design," *Automatica*, Vol. 29, No. 1, 1993, pp. 129–145.

[12]Hyde, R. A., "Meeting Integrated Flight Propulsion Control System Challenges with H_∞," Inst. of Electrical Engineers, IEE Colloquium 015, Feb. 1997.

[13]Härefors, M., "Multivariable Control Design for a Jet Engine," Licentiate of Engineering Thesis, Rept. 203L, Chalmers Univ. of Technology, Gothenburg, Sweden, June 1995.

[14]Härefors, M., "Control Structure Design with Application to Jet Engine," Chalmers Univ. of Technology, TR 009/1999, Gothenburg, Sweden, Aug. 1999.

[15]Shutler, A. G., "Control Configuration Design for the Aircraft Gas Turbine Engine," *Computing and Control Engineering Journal*, Vol. 6, No. 1, 1995, pp. 22–28.

[16]Rubensson, M., "Control Mode Analysis for a Jet Engine," M.Sc. Thesis, Control Engineering Lab., Chalmers Univ. of Technology, Gothenburg, Sweden, May 1997.

[17]Härefors, M., "A Study in Jet Engine Control—Control Structure Selection and Multivariable Design," Ph.D. Thesis 373, Control Engineering Lab., Chalmers Univ. of Technology, Gothenburg, Sweden, Sept. 1999.

[18]Reeves, D. E., "A Comprehensive Approach to Control Configuration Design for Complex Systems," Ph.D. Thesis, Georgia Inst. of Technology, Atlanta, GA, 1991.

[19]Maciejowski, J. M., *Multivariable Feedback Design*, Electronic Systems Engineering Series, Addison Wesley Longman, Reading, MA, 1989.

[20]Manousiouthakis, V., and Nett, C. N., "Euclidian Condition and Block Relative Gain: Connections, Conjectures and Clarifications," *IEEE Transaction on Automatic Control*, Vol. AC-32, No. 5, 1987, pp. 403–407.

[21]Freudenberg, J. S., and Looze, D. P., "Right Half Plane Poles and Zeros and Design Tradeoffs in Feedback Systems," *IEEE Transactions on Automatic Control*, Vol. AC-30, No. 6, 1985, pp. 555–565.

[22]Skogestad, S., and Postlethwaite, I., *Multivariable Feedback Control—Analysis and Design*, Wiley, New York, 1996.

[23]Bristol, E. H., "On a New Measure of Interaction for Multivariable Process Control," *IEEE Transactions on Automatic Control*, Vol. 11, 1966, pp. 133, 134.

[24]Chen, J., Freudenberg, J. S., and Nett, C. N., "The Role of the Condition Number and the Relative Gain Array in Robustness Analysis," *Automatica*, Vol. 30, No. 6, 1994, pp. 1029–1035.

[25]Grosdidier, P., and Morari, M., "Closed-Loop Properties from Steady-State Gain Information," *Industrial and Engineering Chemistry Process Design and Development*, Vol. 24, 1985, pp. 221–235.

[26]Hovd, M., and Skogestad, S., "Simple Frequence-Dependent Tools for Control System Analysis, Structure Selection and Design," *Automatica*, Vol. 28, No. 5, 1992, pp. 989–996.

[27]Hovd, M., and Skogestad, S., "Procedure for Regulatory Control Structure Selection with Application to the FCC Process," *AIChe Journal*, Vol. 39, No. 12, 1993, pp. 1938–1953.

[28]Skogestad, S., and Morari, M., "Implication of Large RGA Elements on Control Performance," *Industrial and Engineering Chemistry Research*, Vol. 26, 1987, pp. 2323–2330.

[29]Manousiouthakis, V., Savage, R., and Arkun, Y., "Synthesis of Decentralized Process Control Structures Using the Concept of Block Relative Gain," *AIChe Journal*, Vol. 32, 1986, pp. 991–1003.

[30]Grosdidier, P., and Morari, M., "Interaction Measures for Systems Under Decentralized Control," *Automatica*, Vol. 22, No. 3, 1986, pp. 309–319.

[31]Doyle, J. C., Glover, K., Khargonekar, P., and Francis, B. A., "State-Space Solution to Standard H2 and H_∞ Control Problems" *IEEE Transactions on Automatic Control*, Vol 34, No. 8, 1989.